ORGANOMETALLICS
Article

Organometallics **2010,** *29,* 2767–2776 2767
DOI: 10.1021/om100236v

Rhodium-Catalyzed Asymmetric Hydroformylation with Taddol-Based IndolPhos Ligands

Jeroen Wassenaar, Bas de Bruin, and Joost N. H. Reek*

Supramolecular & Homogeneous Catalysis, van't Hoff Institute for Molecular Sciences, University of Amsterdam, Nieuwe Achtergracht 166, 1018 WV Amsterdam, The Netherlands

Received March 26, 2010

A small library of Taddol-based IndolPhos ligands **2a**−**g** and their use in asymmetric hydroformylation (AHF) reactions are reported. Moderate to good enantioselectivities are obtained for styrene, vinyl acetate, and allyl cyanide up to 72%, 74%, and 63% ee, respectively. High b/l ratios are obtained, which results in a high net yield of the desired chiral aldehyde. An unprecedented temperature-dependent reversal of enantioselectivity is found when using ligands **2d**,**e**, which are based on a xylyl-derived Taddol in the Rh-catalyzed AHF of styrene. Furthermore, these ligands give the opposite enantiomer of the product for vinyl acetate and allyl cyanide when compared to the other library members, all of which are based on (*R*,*R*)-tartaric acid. Ligands **2a** and **2d** display a similar kinetic profile, which is best described by type I kinetics. Deuterioformylation experiments have shown that insertion of the alkene into the Rh−H bond is irreversible under the conditions applied. High-pressure NMR studies indicate that the hydridobiscarbonyl rhodium species, which is the resting state of the catalyst, features equatorial−apical coordination of the ligands with a preference for the phosphine on the apical position, isomer **A**. However, in the case of ligand **2d** the isomer in which the phosphoramidite occupies the apical position, **B**, is only marginally higher in free energy than isomer **A**. It is proposed that formation of the product takes place via isomer **B** for ligands **2d**,**e** and via isomer **A** for all other ligands, explaining the observed reversal of enantioselectivity.

Introduction

Hydroformylation of alkenes is arguably the most elegant transition metal catalyzed transformation developed to date. In a single reaction step, three substrates (alkene, CO, H_2) are combined to give highly valuable aldehyde products, which may be further transformed by reduction (alcohols), oxidation (acids/esters), or condensation (imines/amines). The 100% atom efficiency of the process has attracted much industrial interest, and nowadays hydroformylation is the largest industrial application of homogeneous catalysis.[1] In most of these processes linear aldehydes are desired, and selective formation of these can be achieved by using wide-bite-angle diphosphine ligands in the case of Rh-catalyzed hydroformylation.[2]

Asymmetric hydroformylation (AHF) on the other hand focuses on formation of the branched aldehydes. As a chiral center is introduced in this reaction, AHF represents a promising tool for the production of optically active compounds for pharmaceutical or agrochemical uses.[3] AHF of styrene derivatives gives rapid access to nonsteroidal anti-inflammatory agents such as ibuprofen, ketoprofen, and naproxen after oxidation of the aldehyde.[3a] When vinyl acetate is used as a substrate, the resulting aldehydes are conveniently transformed into α-amino acids, optically pure isoxazolines, and imidazoles.[4] However, applications to date are rare due to the challenging nature of the reaction. As opposed to other enantioselective reactions such as asymmetric hydrogenation, where only activity and enantioselectivity need to be controlled, AHF also demands a high degree of regiocontrol to suppress the formation of linear aldehydes. Also, generally higher temperatures are required to achieve sufficient reaction rates for AHF, but this often leads to a decrease in regio- and enantioselectivity. Finally, the aldehyde products are prone to racemization under certain reaction conditions.

Over the past two decades a number of chiral phosphorus ligands have been reported, which are able to address these challenges to some extent. Most of these ligands rely on relatively π-acidic phosphorus atoms such as phosphites, phosphoramidites, phospholanes, and diazaphospholanes to achieve good reaction rates as opposed to the electron-rich phosphines most commonly used in asymmetric hydrogenation.

*Corresponding author. Fax: + 31 20 5255604. Tel: + 31 20 5256437. E-mail: j.n.h.reek@uva.nl.

(1) For recent reviews on hydroformylation, see: (a) van Leeuwen, P. W. N. M.; Claver, C. *Rhodium Catalyzed Hydroformylation*; Kluwer Academic Publishers: Dordrecht, 2000; Vol. *22*. (b) Breit, B.; Seiche, W. *Synthesis* **2001**, 1–36. (c) van Leeuwen, P. W. N. M., *Homogeneous Catalysis, Understanding the Art*; Kluwer: Dordrecht, The Netherlands, 2004; pp 125−174.

(2) van Leeuwen, P. W. N. M.; Kamer, P. C. J.; Reek, J. N. H.; Dierkes, P. *Chem. Rev*. **2000**, *100*, 2741–2769.

(3) For reviews on AHF, see: (a) Agbossou, F.; Carpentier, J. F.; Mortreux, A. *Chem. Rev*. **1995**, *95*, 2485–2506. (b) Dieguez, M.; Pamies, O.; Claver, C. *Tetrahedron: Asymmetry* **2004**, *15*, 2113–2122. (c) Klosin, J.; Landis, C. R. *Acc. Chem. Res*. **2007**, *40*, 1251–1259.

(4) Thomas, P. J.; Axtell, A. T.; Klosin, J.; Peng, W.; Rand, C. L.; Clark, T. P.; Landis, C. R.; Abboud, K. A. *Org. Lett*. **2007**, *9*, 2665–2668.

Published on Web 05/27/2010

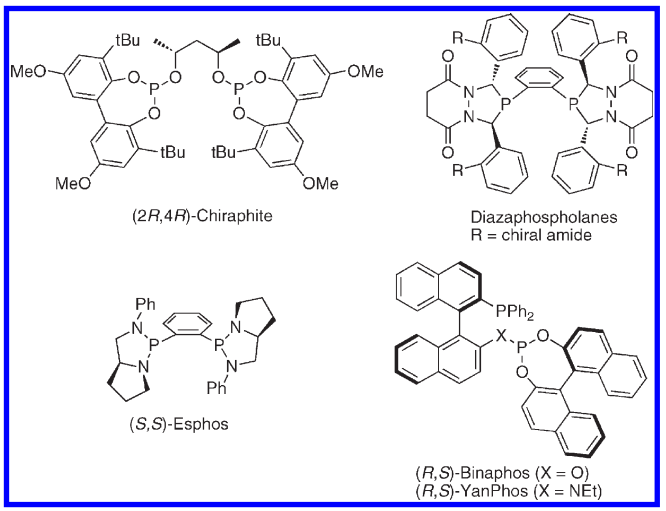

Figure 1. Structure of representative examples of successful ligands for AHF.

Bidentate phosphite ligands such as (2*R*,4*R*)-chiraphite[5] and (*S*,*S*)-kelliphite[6] give high regioselectivities but only moderate ee (Figure 1). C_2-Symmetric phospholane-type ligands, e.g., (*S*,*S*)-Esphos developed by Wills et al., provide high enantioselectivity for vinyl acetate but are unselective for styrene.[7] Landis and Klosin extended the success of phospholane-type ligands with the introduction of diazaphospholanes, giving high ee's for styrene, vinyl acetate, and allyl cyanide.[4,8]

The most promising class of ligands for AHF are hybrid ligands containing a phosphine and a phosphite or phosphoramidite. A major breakthrough was achieved by Takaya and Nozaki with the development of Binaphos and its derivatives, giving ee's up to 94% for a range of substrates.[9] More recently, Zhang and co-workers reported even higher enantioselectivities with their phosphoramidite analogue of Binaphos, YanPhos, giving up to 98% ee for styrene, vinyl acetate, and allyl cyanide.[10] However, both systems give rather low b/l ratios. Other successful examples of phosphine−phosphite systems

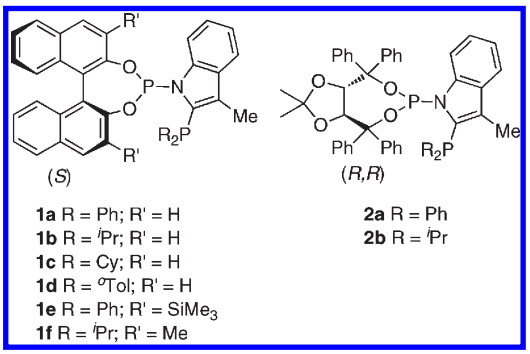

Figure 2. Structures of IndolPhos ligands **1a**−**f** and Taddol-based derivatives **2a**,**b**.

were reported by the groups of van Leeuwen,[11] Dieguez,[12] Pizzano,[13] Schmalz,[14] and Reek.[14,15]

Our group developed hybrid phosphine−phosphoramidite IndolPhos **1** and its Taddol-based derivatives **2** (Figure 2),[16] which have been successfully applied in asymmetric hydrogenation and allylic alkylation. The small bite angle of only 85° observed in the crystal structure of [Rh(**1e**)(cod)]BF_4[16e] prompted us to investigate the use of ligands **1** and **2** in Rh-catalyzed AHF. By virtue of their small bite angle, these ligands would efficiently enforce equatorial−apical coordination in the hydridobiscarbonyl rhodium intermediates, likely leading to a high selectivity for the desired branched aldehyde. Preliminary studies supported this, and high b/l ratios up to 17 along with good enantioselectivity up to 72% ee were obtained.[16a] In this paper a full investigation is reported, focusing on the Taddol-based derivatives **2**. A reversal of enantioselectivity is observed by changing substituents on the Taddol moiety. The origin of this effect has been investigated by kinetic measurements, high-pressure NMR and IR spectroscopy, and DFT calculations.

Results and Discussion

Ligand Synthesis. The Taddol-based IndolPhos derivatives **2a**−**g** are synthesized in a straightforward two-step synthesis from the corresponding (*R*,*R*)-Taddol (Scheme 1). Transformation of the diol into the phosphorochloridite is achieved by treatment with PCl_3 at low temperature under basic conditions. The yields are quantitative, and the phosphorochloridites are used without further purification. Condensation with the corresponding indolylphosphine gives IndolPhos derivatives **2a**−**g** in good yield up to 68% after flash SiO_2 chromatography. The modularity of the synthetic sequence allows for facile derivatization and fine-tuning of the chiral pocket in the corresponding hydroformylation catalysts. The steric and electronic properties have been varied systematically on the phosphine part (**2a**−**c**) and the Taddol moiety (**2d**−**f**), and the effect of substitution of the indole ring on the 7-position has been examined using **2g**. All

(5) (a) Babin, J. E.; Whiteker, G. T. *Asymmetric Synthesis*. World Patent, WO 9303839, 1993. (b) Whiteker, G. T.; Briggs, J. E.; Babin, J. E.; Barner, B. A. Asymmetric Catalysis Using Bisphosphite Ligands. In *Chemical Industries*; Marcel Dekker, Inc.: New York, 2003; Vol. *89*, pp 359−367.

(6) (a) Cobley, C. J.; Gardner, K.; Klosin, J.; Praquin, C.; Hill, C.; Whiteker, G. T.; Zanotti-Gerosa, A.; Petersen, J. L.; Abboud, K. A. *J. Org. Chem.* **2004**, *69*, 4031–4040. (b) Cobley, C. J.; Klosin, J.; Qin, C.; Whiteker, G. T. *Org. Lett.* **2004**, *6*, 3277–3280.

(7) (a) Breeden, S.; Wills, M. *J. Org. Chem.* **1999**, *64*, 9735–9738. (b) Breeden, S.; Cole-Hamilton, D. J.; Foster, D. F.; Schwarz, G. J.; Wills, M. *Angew. Chem., Int. Ed.* **2000**, *39*, 4106–4108.

(8) (a) Landis, C. R.; Jin, W. C.; Owen, J. S.; Clark, T. P. *Angew. Chem., Int. Ed.* **2001**, *40*, 3432. (b) Clark, T. P.; Landis, C. R.; Freed, S. L.; Klosin, J.; Abboud, K. A. *J. Am. Chem. Soc.* **2005**, *127*, 5040–5042.

(9) (a) Nozaki, K.; Sakai, N.; Nanno, T.; Higashijima, T.; Mano, S.; Horiuchi, T.; Takaya, H. *J. Am. Chem. Soc.* **1997**, *119*, 4413–4423. (b) Nozaki, K.; Takaya, H.; Hiyama, T. *Top. Catal.* **1997**, *4*, 175–185.

(10) (a) Yan, Y.; Zhang, X. *J. Am. Chem. Soc.* **2006**, *128*, 7198–7202. (b) Zhang, X.; Cao, B.; Yan, Y.; Yu, S.; Ji, B.; Zhang, X. *Chem.—Eur. J.* **2010**, *16*, 871–877.

(11) (a) Deerenberg, S.; Kamer, P. C. J.; van Leeuwen, P. W. N. M. *Organometallics* **2000**, *19*, 2065–2072. (b) Deerenberg, S.; Pamies, O.; Dieguez, M.; Claver, C.; Kamer, P. C. J.; van Leeuwen, P. W. N. M. *J. Org. Chem.* **2001**, *66*, 7626–7631.

(12) Dieguez, M.; Pamies, O.; Ruiz, A.; Castillon, S.; Claver, C. *Chem.—Eur. J.* **2001**, *7*, 3086–3094.

(13) Rubio, M.; Suarez, A.; Alvarez, E.; Bianchini, C.; Oberhauser, W.; Peruzzini, M.; Pizzano, A. *Organometallics* **2007**, *26*, 6428–6436.

(14) Robert, T.; Abiri, Z.; Wassenaar, J.; Sandee, A. J.; Romanski, S.; Neudorfl, J.-M.; Schmalz, H.-G.; Reek, J. N. H. *Organometallics* **2010**, *29*, 478–483.

(15) Chikkali, S. H.; Bellini, R.; Berthon-Gelloz, G.; van der Vlugt, J. I.; de Bruin, B.; Reek, J. N. H. *Chem. Commun.* **2010**, *46*, 1244–1246.

(16) (a) Wassenaar, J.; Reek, J. N. H. *Dalton Trans.* **2007**, 3750–3753. (b) Wassenaar, J.; Kuil, M.; Reek, J. N. H. *Adv. Synth. Catal.* **2008**, *350*, 1610–1614. (c) Wassenaar, J.; Reek, J. N. H. *J. Org. Chem.* **2009**, *74*, 8403–8406. (d) Wassenaar, J.; van Zutphen, S.; Mora, G.; Le Floch, P.; Siegler, M. A.; Spek, A. L.; Reek, J. N. H. *Organometallics* **2009**, *28*, 2724–2734. (e) Wassenaar et al. *Chem. Eur. J.* **2010**, DOI: 10.1002/chem.200903476.

Scheme 1. Synthesis of Taddol-Based IndolPhos Ligands 2a−g

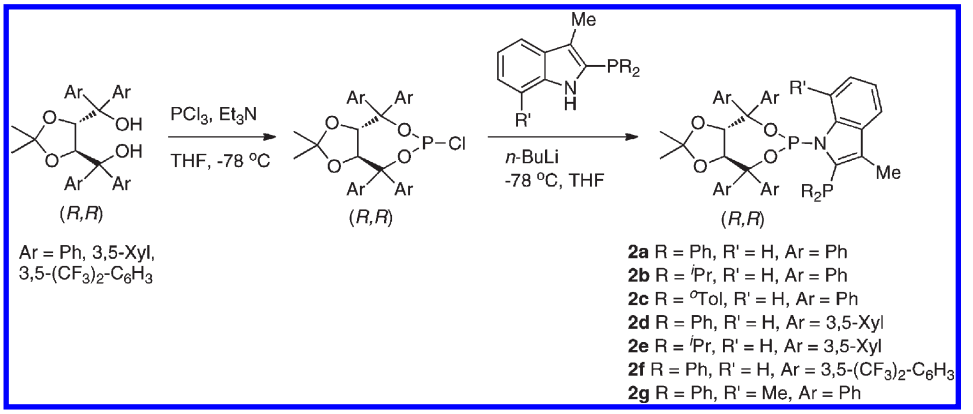

ligands are easy to handle as white powders and are stable as a solid toward air and moisture.

Similar to the bisnaphthol-based IndolPhos ligands **1**, the Taddol-based derivatives display large coupling constants between the two inequivalent phosphorus atoms in the ^{31}P NMR spectra ($J_{PP} \approx 200$ Hz). In the case of isopropyl phosphines (**2b** and **2e**), two conformations of the ligand are observed at low temperatures of which only one displays a P−P coupling. We believe that this is due to rotation of the phosphine−carbon bond, leading to two conformers where the phosphorus lone pairs point toward each other or away from one another. In the former case a large coupling constant is expected but not in the latter.

Ligand Screening in AHF. Preliminary experiments in the AHF of styrene using IndolPhos ligands **1** showed that only the isopropyl-substituted ligands **1b**,**f** were giving appreciable levels of activity and regio- and enantioselectivity.[16a] In the case of phenyl-substituted ligands no conversion was obtained, which is likely explained by the formation of bis-ligated species, as has been observed for TangPhos systems.[16a,17] The more bulky Taddol-based ligands should not suffer from this problem, and indeed active catalysts are generated with all ligands. Styrene was used as benchmark substrate, and ligand screening was carried out under standard conditions (20 bar of CO/H_2, PhMe, L/Rh = 2.0) at 40 and 70 °C (Table 1). Even though higher rates can be expected at lower syngas pressures, we chose 20 bar, as lower pressures may have a detrimental effect on the enantioselectivity and conversion due to slow formation of the active species (*vide infra*).

Taddol-based ligand **2a** provides the hydroformylation product of styrene in 71% ee, which is almost identical to bisnaphthol-based ligand **1b** (entries 3 and 5). However, the regioselectivity is much higher (b/l ratio of 28) and the conversion somewhat lower. Increasing the steric bulk on the phosphine moiety leads to a decrease in activity, regioselectivity, and enantioselectivity (entries 7 and 9). The use of more bulky xylyl paddlewheels on the Taddol fragment leads to a decrease in activity and enantioselectivity, but raises the b/l ratio up to 37 (entries 11 and 13). At 40 °C, only traces of hydroformylation products were obtained employing the perfluorated ligand **2f** (entry 15). We found previously that substituents on the ligand backbone of Taddol-containing phosphine−phosphite ligands dramatically enhanced the enantioselectivity in the AHF of styrene.[14] However, ligand **2g**, containing a methyl group in the 7-position of the indole backbone, gives a lower activity, b/l ratio, and ee (entry 17).

Table 1. Screening of Ligands in AHF of Styrene[a]

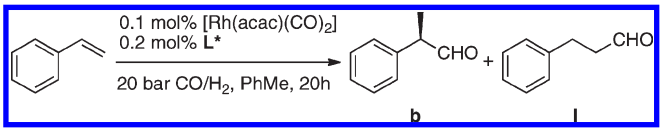

entry	ligand	*T* (°C)	% conv[b]	b/l[c]	% ee[d]
1	**1a**	40	32	14	64 (*R*)
2		70	99	6	46 (*R*)
3	**1b**	40	96	10	72 (*R*)
4		70	100	6	53 (*R*)
5	**2a**	40	57	28	71 (*R*)
6		70	100	14	46 (*R*)
7	**2b**	40	3	14	55 (*R*)
8		70	69	10	44 (*R*)
9	**2c**	40	8	2	48 (*R*)
10		70	98	21	42 (*R*)
11	**2d**	40	48	37	33 (*R*)
12		70	100	20	16 (*S*)
13	**2e**	40	8	17	37 (*R*)
14		70	100	5	10 (*S*)
15	**2f**	40	< 1		
16		70	98	21	11 (*S*)
17	**2g**	40	10	5	58 (*R*)
18		70	100	6	3 (*R*)

[a] [Rh(acac)(CO)$_2$] = 1.0 mmol/L in toluene, [ligand] = 2.0 mmol/L, styrene/rhodium = 1000, pressure = 20 bar (CO/H_2 = 1:1). [b] Percentage conversion determined by GC; the reaction was stopped after 20 h. [c] Ratio of branched to linear product. [d] Enantiomeric excess determined by chiral GC (Supelco BETA DEX 225).

When the temperature is raised to 70 °C, almost all ligands provide catalysts that give full conversion, but both enantioselectivity and regioselectivity are significantly lower. Remarkably, raising the temperature from 40 to 70 °C, when applying ligands **2d** and **2e**, reverses the enantioselection from *R* (37% ee) to *S* (up to 16% ee, entries 11−14). This result is highly unexpected and has up to now been observed only in Pt/Sn-catalyzed AHF reactions.[18] It may be caused by the presence of multiple active isomers of the catalyst, with a temperature dependent relative distribution and/or a different response of these isomers in rate to temperature changes. The phenomenon will be discussed in more detail below.

(17) Axtell, A. T.; Klosin, J.; Abboud, K. A. *Organometallics* **2006**, *25*, 5003–5009.

(18) (a) van Duren, R.; Cornelissen, L. L. J. M.; van der Vlugt, J. I.; Huijbers, J. P. J.; Mills, A. M.; Spek, A. L.; Müller, C.; Vogt, D. *Helv. Chim. Acta* **2006**, *89*, 1547–1558. (b) Tóth, I.; Guo, I.; Hanson, B. E. *Organometallics* **1993**, *12*, 848–852.

Table 2. Screening of Ligands in AHF of Vinyl Acetate[a]

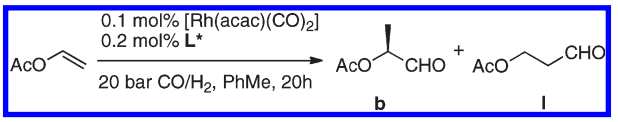

entry	ligand	T (°C)	% conv[b]	b/l[c]	% ee[d]
1	**1a**	40	2	1.2	24 (*S*)
2		70	100	16.8	19 (*S*)
3	**1b**	40	5	4.2	31 (*S*)
4		70	97	777	42 (*S*)
5	**2a**	40	19	21.7	72 (*S*)
6		70	98	40	33 (*S*)
7	**2b**	40	< 1		
8		70	49	199	36 (*S*)
9	**2c**	40	< 1		
10		70	87	25.7	6 (*R*)
11	**2d**	40	13	8	59 (*R*)
12		70	99	97	35 (*R*)
13	**2e**	40	2	0.3	39 (*R*)
14		70	49	59	29 (*R*)
15	**2f**	40	< 1		
16		70	99	1.5	10 (*S*)
17	**2g**	40	2	0.3	51 (*S*)
18		70	100	15.1	< 2

[a] $[Rh(acac)(CO)_2] = 1.0$ mmol/L in toluene, [ligand] = 2.0 mmol/L, vinyl acetate/rhodium = 1000, pressure = 20 bar (CO/H_2 = 1:1). [b] Percentage conversion determined by GC; the reaction was stopped after 20 h. [c] Ratio of branched to linear product. [d] Enantiomeric excess determined by chiral GC (Supelco BETA DEX 225).

Table 3. Screening of Ligands in AHF of Allyl Cyanide[a]

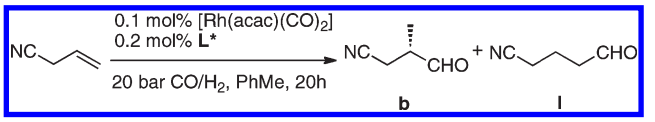

entry	ligand	T (°C)	% conv[b]	b/l[c]	% ee[d]
1	**1a**	40	10	50	51 (*S*)
2		70	3	16.5	45 (*S*)
3	**1b**	40	78	8.4	63 (*S*)
4		70	99	6.3	55 (*S*)
5	**2a**	40	71	4.4	59 (*S*)
6		70	99	3.2	50 (*S*)
7	**2b**	40	6	4.8	40 (*S*)
8		70	96	2.1	36 (*S*)
9	**2c**	40	12	1.2	45 (*S*)
10		70	98	1.0	43 (*S*)
11	**2d**	40	39	4.1	35 (*R*)
12		70	99	3.3	29 (*R*)
13	**2e**	40	8	4.1	47 (*R*)
14		70	98	2.3	39 (*R*)
15	**2f**	40	4	8.4	24 (*S*)
16		70	98	2.3	17 (*S*)
17	**2g**	40	14	3.5	37 (*S*)
18		70	99	2.4	3 (*S*)

[a] $[Rh(acac)(CO)_2] = 1.0$ mmol/L in toluene, [ligand] = 2.0 mmol/L, allyl cyanide/rhodium = 1000, pressure = 20 bar (CO/H_2 = 1:1). [b] Percentage conversion determined by GC; the reaction was stopped after 20 h. [c] Ratio of branched to linear product. [d] Enantiomeric excess determined by chiral GC (Astec Chiraldex A-TA).

To study the scope, we applied IndolPhos ligands **1** and **2** in the AHF of vinyl acetate (Table 2). Bisnaphthol-based ligands **1a**,**b** yield unreactive and unselective catalysts for this substrate, as conversions of only up to 5% at low b/l ratios and ee are achieved (entries 1 and 3). Conversely, Taddol-based ligand **2a** leads to moderate rates and a good ee of 72% and b/l ratio of 22, similar to the performance in the case of styrene (entry 5). Surprisingly, the xylyl-functionalized ligand **2d** gives the opposite enantiomer in 59% ee (entry 11, $\Delta ee = 141\%$). Both ligands contain the same absolute configuration of the Taddol moiety (*R*,*R*) and differ only in substituents on the paddlewheels. Such a dramatic reversal of absolute configuration induced by a slight modification of the substituents on the ligand in AHF reactions has been observed only for Josiphos ligands ($\Delta ee \leq 82\%$).[17] The other ligands display very low activities at 40 °C. At 70 °C, most ligands give quantitative conversion, except for the more bulky isopropyl- and *o*-tolyl-functionalized ligands **2b**, **2c**, and **2e**. The b/l ratio increases at higher temperatures, which in some cases leads to almost exclusive formation of the branched product with a b/l ratio up to 777 (entries 4 and 8). The enantioselectivity is generally lower at higher temperature, but remarkably, the application of ligand **1b** at higher temperature results in an increase of ee (from 31% to 42%, entry 4).

AHF of allyl cyanide is a potentially valuable process, as it furnishes β-amino acid derivatives after hydrogenation and oxidation. Application of IndolPhos ligands **1** and **2** in this reaction lead to b/l ratios up to 50% and 63% ee at high conversion (Table 3). In general b/l ratios for this substrate are low, and the regioselectivity provided by ligand **1a** is exceptional and among the highest reported to date. The absolute configuration also reverses for this substrate when using the more sterically demanding xylyl-functionalized ligands **2d** and **2e**, similar to the case of vinyl acetate (entries 11−14).

Summarizing, the ligand screening experiments in the AHF of three substrates gave enantioselectivities up to 72%, 72%, and 63% ee for styrene, vinyl acetate, and allyl cyanide, respectively. Using the full library of IndolPhos ligands **1** and **2**, the substrate specificity of the generated catalysts is low, making them attractive for general use. The enantioselectivities are not among the highest reported but certainly useful as the ee of commercially relevant products may be increased by crystallization. Especially the high b/l ratios result in a high net yield of the desired optically active branched aldehyde. The dependence of the absolute configuration of the products on the temperature and substituents on the ligand is unexpected and up to now unexplored in the literature. Understanding these effects may lead to a better mechanistic picture and eventually a route to rational optimization of the catalysts. Therefore kinetic studies, high-pressure NMR experiments, and DFT calculations were performed to uncover the origin of the enantioreversal.

Kinetics. In order to determine whether the catalysts generated from ligands **2a** and **2d** follow the same catalytic cycle, we monitored the progress of the AHF of vinyl acetate in time using *in situ* gas uptake measurements. The rate-determing step in hydroformylation reaction can be early or late in the catalytic cycle, leading to type I or type II kinetics, respectively (eqs 1 and 2).

$$\text{rate(type I)} = \frac{A[\text{alkene}][\text{Rh}]}{B + [\text{L}]} \quad (1)$$

$$\text{rate(type II)} = \frac{C[\text{H}_2][\text{Rh}]}{D + [\text{CO}]} \quad (2)$$

($A-D$ are constants, [L] is proportional to the [phosphine ligand] and [CO]).

In type I kinetics, positive orders are found in [alkene] and [rhodium], a zero order in $p\text{H}_2$, and a negative order in the [ligand] and/or pCO. Most catalyst systems follow these kinetics, which is consistent with a rate-determining alkene

Table 4. Influence of Syngas Pressure on the Asymmetric Hydroformylation of Vinyl Acetate with Ligands 2a and 2d[a]

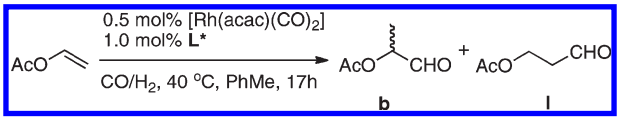

entry	ligand	$P_{CO/H2}$ (bar)	% conv[b]	TOF (h^{-1})[c]	b/l[d]	% ee[e]
1	**2a**	10	51	7.6	58.7	73 (*S*)
2		20	23	3.5	19.0	73 (*S*)
3		30	20	3.1	14.3	74 (*S*)
4		40	16	2.5	9.9	73 (*S*)
5	**2d**	10	37	6.5	21.4	58 (*R*)
6		20	23	3.5	12.0	59 (*R*)
7		30	15	2.7	9.6	60 (*R*)
8		40	11	2.2	5.4	59 (*R*)

[a] [Rh(acac)(CO)$_2$] = 1.0 mmol/L in toluene, [ligand] = 2.0 mmol/L, vinyl acetate/rhodium = 200, temperature = 40 °C. [b] Percentage conversion determined by GC; the reaction was stopped after 17 h. [c] Turnover frequency determined in the linear part of the reaction profile (10−20% conv). [d] Ratio of branched to linear product. [e] Enantiomeric excess determined by chiral GC (Supelco BETA DEX 225).

coordination or migratory insertion of the alkene in the Rh−H bond. Type II kinetics has been reported for bulky phosphite systems, giving fast catalysts in which oxidative addition of H_2 to the acylrhodium species is rate determining, hence a positive order in pH_2. In type I kinetics the enantioselectivity is determined in the migratory insertion under conditions where this step is irreversible.[1a,19]

Table 4 summarizes the performance of ligands **2a** and **2d** in the hydroformylation of vinyl acetate. The enantioselectivity is independent of the pressure, whereas the b/l ratio is lower at higher syngas pressures. The latter is unexpected, as usually higher CO pressures result in higher b/l ratios.[1a] Also the conversion is lower at higher pressures, thus indicating a negative order in *p*CO.

The lower rates at higher pressures are also reflected in the reaction profiles derived from gas uptake measurements (Figure 3). Turnover frequencies are obtained from these profiles, which are given in Table 4. A significant decrease of the rate is observed with increasing pressure, again in line with the negative order in *p*CO. At 10 bar the curves show an induction period up to 4 h, most likely resulting from slow formation of the active hydridobiscarbonyl species from the acac complex. At higher pressures, the active species is formed faster and no induction period is observed. After the induction period, a constant slope is observed for both ligands, indicating steady-state kinetics up to at least 50% conversion. This can be explained by reversible alkene coordination prior to an irreversible migratory insertion, which results in a pseudo-zero-order in [alkene] at high concentrations of the substrate. Ligand **2a** gives a slightly higher rate compared to ligand **2d**, an effect that is more pronounced at lower pressures.

The kinetics observed for both systems above are in best agreement with type I kinetics, as we found a strong decrease in rate with increasing syngas pressure. The rate-determining step is proposed to be the migratory insertion because steady-state kinetics are observed in the beginning of the reaction, indicating reversible alkene coordination. The absolute configuration is determined in the insertion step, if this step is irreversible.

(19) Horiuchi, T.; Shirakawa, E.; Nozaki, K.; Takaya, H. *Organometallics* **1997**, *16*, 2981–2986.

To investigate whether insertion of the alkene is reversible, we carried out deuterioformylation experiments with vinyl acetate using a CO/D_2 (1:1) gas mixture. Under standard conditions similar conversions and higher b/l ratios are observed (Scheme 2). The pathway leading to the linear aldehyde is less favorable when deuterium is used, as was also observed for Binaphos by Nozaki and Takaya.[19] The ee is not significantly affected by the use of D_2 instead of H_2. Analysis of the products by ^{1}H NMR shows that deuterium is incorporated only at the expected positions, i.e., on the aldehyde and methyl groups. Since no scrambling of the deuterium atoms occurs, the insertion of the alkene in the Rh−H bond is irreversible under the applied conditions.[19]

High-Pressure NMR and IR Spectroscopy. The hydridobiscarbonyl species of all Taddol-based IndolPhos ligands **2** were studied by high-pressure ^{1}H and ^{31}P NMR spectroscopy. As a reference, bisnaphthol-based ligand **1a** was also used in this study. Three different isomers can be expected for unsymmetrical hybrid ligands, the ee (bis-equatorial) isomer and two ea (equatorial−apical) isomers, **A** and **B**, in which either the phosphine or the phosphoramidite occupies the apical position (Figure 4). The complexes were generated in a high-pressure NMR tube from the corresponding acac complex that was exposed to 5 bar of CO/H_2 at 50 °C for 16 h. The chemical shifts of the hydride and phosphorus signals as well as the coupling constants with the hydride are depicted in Table 5. Ligand **2c** gave rise to the formation of a new species under syngas atmosphere observed by ^{31}P NMR; however, no hydride signal could be detected. In the case of ligand **2g** only decomposition was observed after prolonged heating under syngas atmosphere.

The metal complexes of all ligands (except for **2c** and **2g**) give rise to either a doublet-of-doublets-of-doublets or a doublet-of-triplets (in case one of the hydride−phosphorus couplings equals the Rh−H coupling constant) in the ^{1}H NMR spectrum at high field (−8−10 ppm). No other hydride signals were detected under the indicated conditions. At least one of the hydride−phosphorus couplings is very large, which is indicative for a *trans* disposition of hydride and the phosphorus atom. This observation already excludes formation of ee complexes, which is in line with what we expected on the basis of the small bite-angle of the ligand. The Rh−H coupling constant is around 8−10 Hz, typical for trigonal-bipyramidal [Rh(H)(CO)$_2$(L)$_2$] complexes.

Bisnaphthol-based ligand **1a** exhibits large values for the $^2J_{HP(phosphine)}$ and $^2J_{HP(phosphoramidite)}$ couplings, in which the latter is the largest one (Table 5, entries 1, 2). This indicates a rapid equilibrium between isomers **A** and **B**, in which **B** is the major species.[20] The temperature dependence of the $^2J_{HP}$ couplings confirms this proposition. For the Taddol-based ligands, an opposite trend is observed with large values for $^2J_{HP(phosphine)}$, indicating a preference for isomer **A** (Table 5, entries 3−14). The temperature-dependent coupling constants allow calculation of the ratio between **A** and **B**, which is >99:1 at 45 °C.[20] The more bulky xylyl-functionalized Taddol in ligands **2d** and **2e** gives rise to slightly larger values of $^2J_{HP(phosphoramidite)}$ compared to the ligands containing the parent Taddol. This indicates that the equilibrium between **A** and **B** is slightly shifted toward isomer **B** for the more bulky ligand **2d** (**A**/**B** = 95:5 at 45 °C), which is also reflected in the

(20) Casey, C. P.; Paulsen, E. L.; Beuttenmueller, E. W.; Proft, B. R.; Petrovich, L. M.; Matter, B. A.; Powell, D. R. *J. Am. Chem. Soc.* **1997**, *119*, 11817–11825.

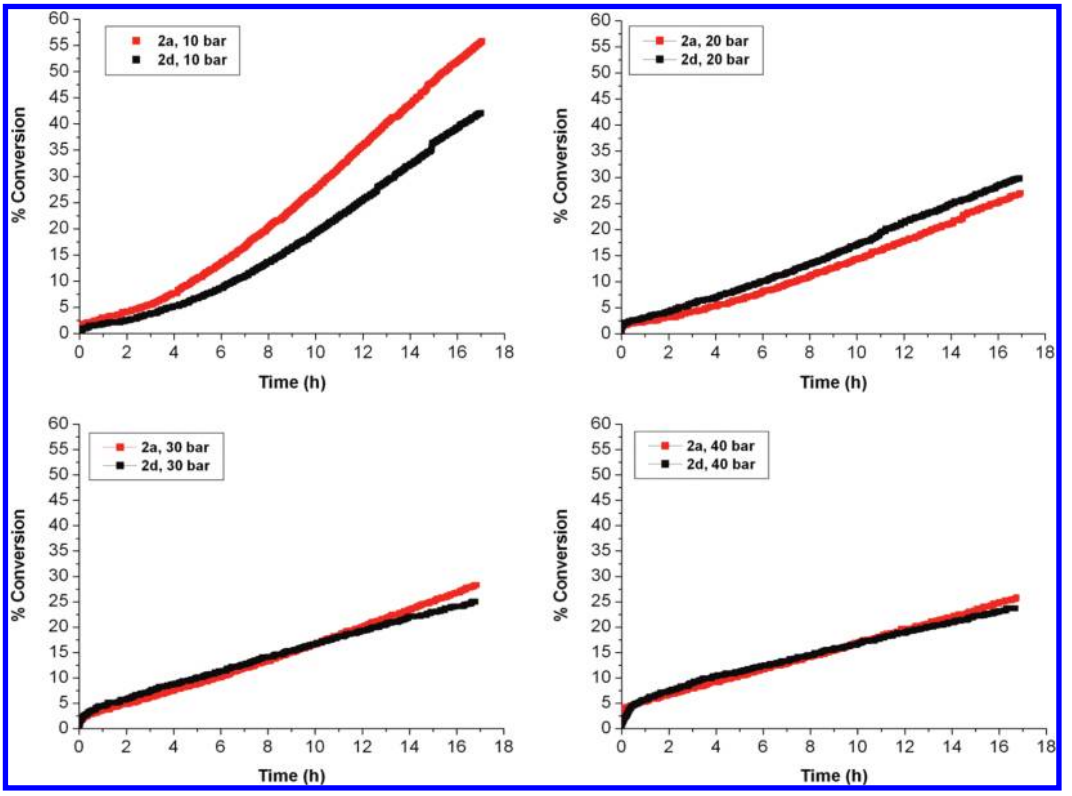

Figure 3. Reaction profiles of the asymmetric hydroformylation of vinyl acetate using ligands **2a** and **2d** at 10, 20, 30, and 40 bar of CO/H_2 and 40 °C. Conversions are obtained from gas uptake curves using the ideal gas law and are uncorrected. Dissolution of the gas into the solution is not entirely finished at the point of reaction start, leading to slightly higher conversions than obtained by GC.

Scheme 2. Deuteroformylation of Vinyl Acetate with Ligands 2a and 2d

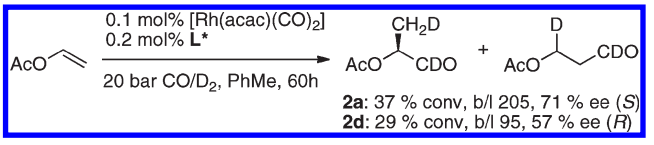

smaller energy difference between these species found by DFT calculations (*vide infra*).

For hybrid phosphine−phosphoramidite ligands, no high-pressure NMR studies of the hydridobiscarbonyl rhodium species have been reported so far. For phosphine−phosphites on the other hand, examples have been reported with a preference both for isomer **A** (van Leeuwen,[11a] Claver,[21] Pizzano,[13] Schmalz and Reek[14]) and for isomer **B** (Binaphos[9a]). The presence of both isomers **A** and **B** in the case of IndolPhos ligands **2a** and **2d** raises the question, which will be the active species leading to the product? In analogy to the mechanism of asymmetric hydrogenation, the minor isomer **B** may be far more active, resulting from a lower transition-state barrier for alkene insertion than **A** and thus leading to the product.

High-pressure *in situ* IR spectroscopy enables the study of the catalyst resting state during the reaction, giving valuable mechanistic information.[22] We studied the formation of the hydridobiscarbonyl rhodium species for ligands **2a** and **2d**, which were formed within 20 h at 40 °C and 20 bar of CO/H_2 in cyclohexane (Figure 5). As expected, only one set of signals

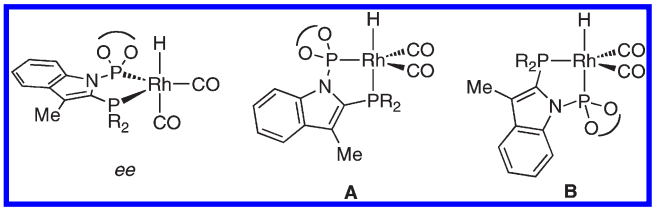

Figure 4. Structures of bis-equatorial isomer ee and equatorial−apical isomers **A** and **B** of the hydridobiscarbonyl rhodium species.

Table 5. NMR Data for the Hydride Resonance of RhH(IndolPhos)$(CO)_2$ Complexes[a]

entry	ligand	T (°C)	δ_{HRh}	$^1J_{RhH}$	δ_{PC}	$^2J_{HPC}$	δ_{PN}	$^2J_{HPN}$
1	**1a**	25	−8.40	9.9	68.2	66.7	176.7	95.7
2		45	−8.48	9.7	68.5	63.8	176.9	101.9
3	**2a**	25	−8.78	9.5	29.7	113.1	144.0	3.6
4		45	−8.82	9.4	29.8	112.7	143.8	4.8
5	**2b**	25	−8.35	9.1	69.3	109.1	142.5	nd[b]
9	**2d**	25	−8.62	9.6	29.5	110.5	142.2	9.6
10		45	−8.69	9.6	29.5	109.2	142.2	12.3
11	**2e**	25	−8.26	10.0	69.1	108.4	140.4	6.2
12		45	−8.34	8.7	69.1	107.6	140.4	8.7
13	**2f**	25	−9.64	9.7	nd[c]	111.0	nd[c]	2.3
14		45	−9.67	8.6	nd[c]	112.3	nd[c]	nd[b]

[a] Hydridobiscarbonyl complexes were generated from [Rh(acac)$(CO)_2$] and the corresponding ligand by heating for 16 h at 50 °C under 5 bar of CO/H_2 in C_6D_6. [b] Not detected due to zero or near zero value of coupling constant. [c] Not detected due to low concentration.

(symmetric and antisymmetric stretch) for the carbonyls of the ea complex is observed in both cases. The calculated IR absorptions (ri-DFT, BP86, SV(P)) of isomer **A** for ligand **2a** (2016.9

(21) Pamies, O.; Net, G.; Ruiz, A.; Claver, C. *Tetrahedron: Asymmetry* **2002**, *12*, 3441–3445.
(22) Kamer, P. C. J.; van Rooy, A.; Schoemaker, G. C.; van Leeuwen, P. W. N. M. *Coord. Chem. Rev.* **2004**, *248*, 2409–2424.

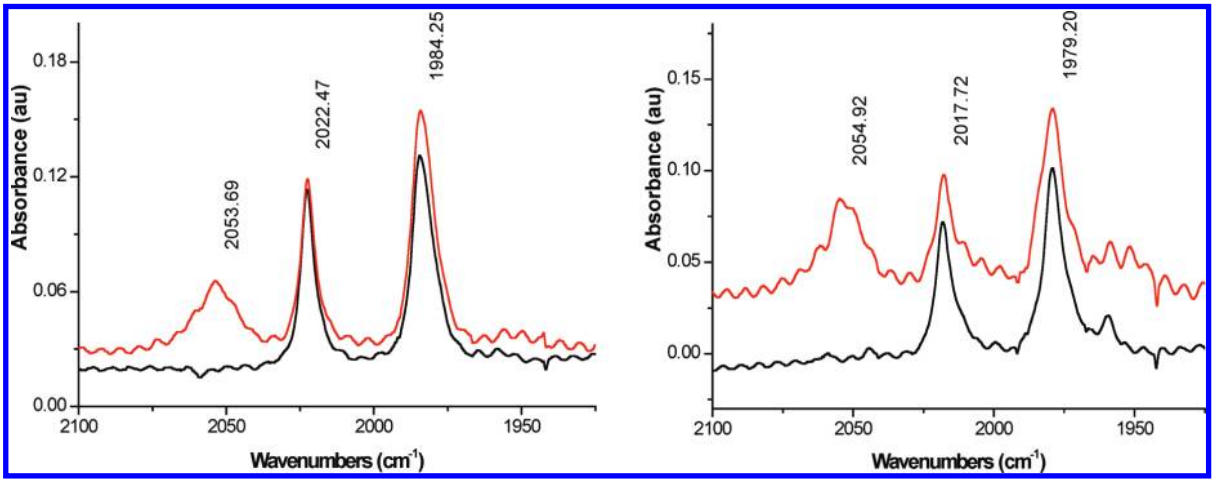

Figure 5. High-pressure IR spectra of RhH(IndolPhos)$(CO)_2$ complexes of ligands **2a** (left) and **2d** (right) after incubation (black) and in the presence of vinyl acetate (red).

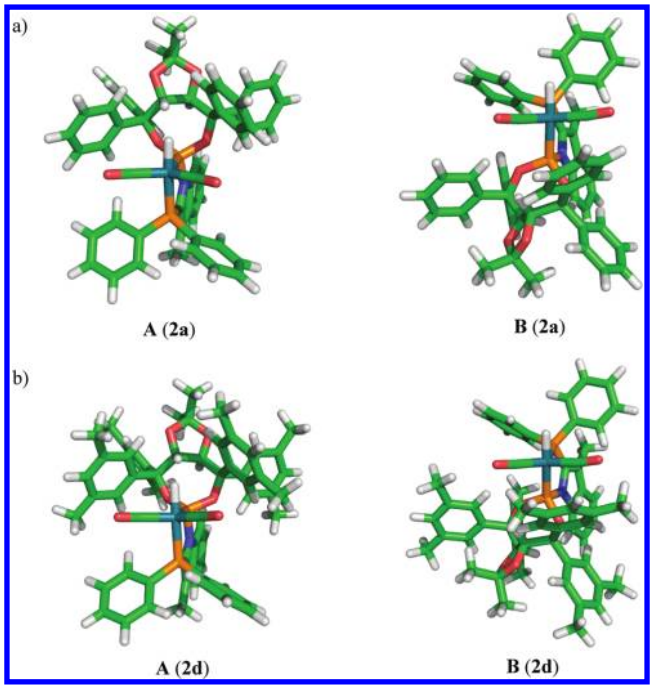

Figure 6. DFT-calculated structures of isomers **A** and **B** with (a) ligand **2a** and (b) ligand **2d**.

and 1990.2 cm^{-1}) and **2d** (2012.0 and 1984.6 cm^{-1}) correspond well with the experimentally found absorptions (**2a**: 2022.5 and 1984.3 cm^{-1}; **2b**: 2017.7 and 1979.2 cm^{-1}). Visualization of the computed CO vibrations of isomer **A** for both ligands reveals that they are strongly coupled with the Rh−H stretching modes. The observation of only one set of signals indicates that the carbonyl ligands of isomer **A** dominate the spectrum. Isomer **B** seems to be visible in small amounts as red-shifted shoulders partly overlapping the main signals of isomer **A**. The shoulders are more pronounced for **2d**, in agreement with the NMR data. Upon addition of vinyl acetate, a second species forms in both experiments at slightly higher wavenumbers (±2054 cm^{-1}), exhibiting only a single peak. This signal is unlikely to stem from a monocarbonyl alkene adduct, [RhH(**2a**)(CO)(vinyl acetate)]. Calculation of those complexes gave IR absorptions at much lower wavenumbers, as is to be expected. Instead, it seems that the substrate induces the formation of a dormant species that is in equilibrium with the active species. In line with this, the signal disappears slowly as the reaction proceeds. The nature of this dormant species is currently not clear.

Table 6. Calculated Energies of Hydridobiscarbonyl Rhodium Isomers A and B for Ligands 2a and 2d at the ri-DFT BP86 Level Using the SV(P) Basis Set on All Atoms[a]

entry	ligand	isomer	T (°C)	ΔE_{ZPE}[b]	ΔG[c]	ΔH[d]	ΔS[e]
1	**2a**	**A**	25	0.0	0.0	0.0	0.0
2		**B**	25	3.1	3.4	3.3	−0.5
3		**A**	40	0.0	0.0	0.0	0.0
4		**B**	40	3.1	3.3	3.3	−0.2
5	**2d**	**A**	25	0.0	0.0	0.0	0.0
6		**B**	25	2.5	0.1	2.4	7.8
7		**A**	40	0.0	0.0	0.0	0.0
8		**B**	40	2.5	−0.1	2.5	8.5

[a] All energies are relative to isomer **A** for each ligand at each temperature. [b] Zero point energy corrected SCF energy in kcal/mol. [c] Standard free energy difference in the gas phase (1 bar), in kcal/mol. [d] Standard enthalpy difference in the gas phase in kcal/mol. [e] Standard entropy difference in the gas phase in cal/mol/K.

DFT Calculations. In order to gain a more detailed understanding of the relative energies of isomers **A** and **B** for ligands **2a** and **2d**, and to assign the IR spectra more accurately, we carried out DFT calculations on these complexes. The calculated structures for the RhH(IndolPhos)$(CO)_2$ species of ligands **2a** and **2d** are displayed in Figure 6a, b, respectively. The energies are summarized in Table 6.

The geometries obtained after optimization for isomers **A** and **B** are very similar for both ligands. The increased steric bulk of the xylyl-substituted ligand **2d** does not lead to a large conformational change. Conversely, the steric bulk of **2d** has a major impact on the stability of the two isomers, as the energy difference between **A** and **B** is much smaller for ligand **2d** compared to **2a**. For **2a**, isomer **A** is 3.4 kcal/mol more stable, which is also reflected in the small fraction of **B** (< 1%) found by HP-NMR. For **2d**, isomer **B** is almost equal in free energy to **A**. This is in good agreement with the HP-NMR studies, where larger values for $^2J_{HP(phosphoramidite)}$ were found in the case of ligand **2d**, and about 5% of isomer **B** is present in solution at 45 °C. The slightly larger energy difference found spectroscopically may be attributed to solvent effects. Moreover, a positive entropy contribution is observed for conversion of **A** (**2d**) to **B** (**2d**) versus a negative contribution in the case of conversion of **A**

Scheme 3. Mechanism of Enantioselection of Ligands 2a (left) and 2d (right) Leading to the Opposite Enantiomers of the Product

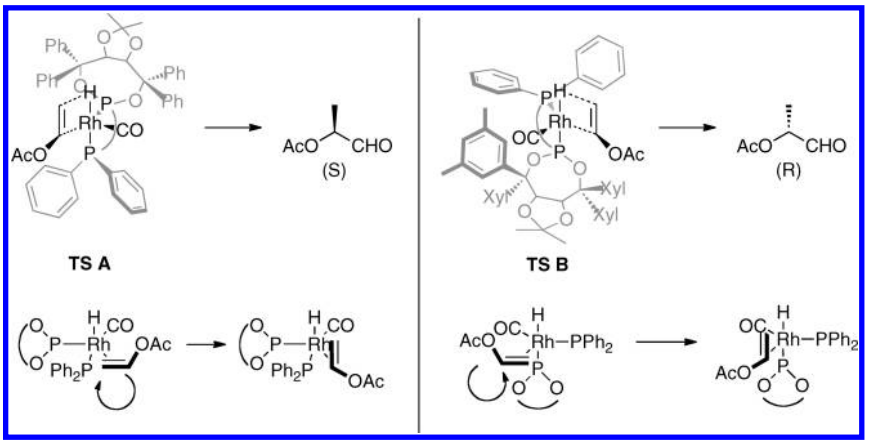

(**2a**) to **B** (**2a**). This may explain the temperature-dependent reversal of enantioselectivity when styrene is used as a substrate (Table 1).

Proposed Mechanism of Enantiodiscrimination. On the basis of the results outlined above, it can be envisioned that the reversal of enantioselectivity observed in the asymmetric hydroformylation using ligands **2a** and **2d** is a result of the difference in relative stability of ea isomers **A** and **B** for ligands **2a** and **2d**. The migratory insertion of the alkene into the Rh−H bond, which is proposed to be the rate- and selectivity-determining step (*vide supra*), is accompanied by a rotation of the double bond from in-plane coordination to a perpendicular mode in the transition state. For ligand **2a** the reaction may proceed via hydridobiscarbonyl rhodium species **A**, which, after loss of one molecule of CO, selectively coordinates the alkene, which inserts into the Rh−H bond in TS **A** (Scheme 3). The configuration of the phenyl rings on the phosphine, controlled by the chiral information in the Taddol moiety, blocks the double-bond rotation selectively, similarly to that proposed by Pizzano et al.[13] In the case of ligand **2d** the main reaction flux may be carried by isomer **B** and the selectivity is determined in TS **B**. One of the xylyl paddlewheels of the Taddol moiety selectively blocks one coordination site. The other site can selectively discriminate between the two prochiral faces of the olefin. However, when the substituent on the olefin becomes larger, as is the case in styrene, the substrate does not fit very well, and reaction via TS **A** becomes competitive. Only by shifting the equilibrium to isomer **B** using higher temperatures (ΔS is positive) can TS **B** dominate the outcome of the reaction.

The proposed mechanism assumes similar barriers for alkene insertion for both isomers **A** and **B**. However, it is known that in many reactions the minor species may lead to the product, like in asymmetric hydrogenation. Therefore, calculation of these transition states is necessary to give a definitive answer. Nonetheless, the proposed mechanism is in accordance with all data obtained by experimental and theoretical techniques.

Conclusions

Summarizing, we have reported the synthesis of a small library of Taddol-based IndolPhos ligands and their use in AHF reactions. Moderate to good enantioselectivities are obtained for styrene, vinyl acetate, and allyl cyanide up to 72%, 74%, and 63% ee, respectively. High b/l ratios are obtained, which results in a high net yield of the desired chiral aldehyde. We found an unprecedented temperature-dependent reversal of enantioselectivity using ligands **2d**−**e**, which are based on a xylyl-derived Taddol in the Rh-catalyzed AHF of styrene. Furthermore, these ligands give the opposite enantiomer of the product for vinyl acetate and allyl cyanide when compared to the other library members, all of which are based on (*R*,*R*)-tartaric acid.

We investigated the origin of this enantioreversal by kinetic studies, high-pressure NMR and IR, and DFT calculations. It was found that ligands **2a** and **2d** reveal a similar kinetic profile, which is best described by type I kinetics. Deuterioformylation experiments have shown that insertion of the alkene into the Rh−H bond is irreversible under the conditions applied. The hydridobiscarbonyl rhodium species, which is the resting state of the catalyst, features equatorial−apical coordination of the ligands with a preference for the phosphine on the apical position, isomer **A**. However, DFT calculations and high-pressure NMR studies indicate that in the case of ligand **2d** the isomer in which the phosphoramidite occupies the apical position, **B**, is only marginally higher in free energy than isomer **A**. We therefore propose that formation of the product takes place via isomer **B** for ligands **2d**−**e** and via isomer **A** for all other ligands, explaining the observed reversal of enantioselectivity.

In conclusion, we have demonstrated the efficient applicability of catalysts derived from Taddol-based IndolPhos ligands in AHF reactions. Moreover, the detailed investigation triggered by an unprecedented reversal of enantioselectivity has provided valuable insights into the mechanism of enantiodiscrimination in AHF reactions that may also be applicable for other catalytic systems.

Experimental Section

General Procedures. All reactions were carried out under an atmosphere of argon using standard Schlenk techniques. THF, pentane, hexane, and diethyl ether were distilled from sodium benzophenone ketyl; CH_2Cl_2, 2-propanol, and methanol were distilled from CaH_2; and toluene was distilled from sodium under nitrogen. With the exception of the compounds given below, all reagents were purchased from commercial suppliers and used without further purification. The following compounds were synthesized according to published procedures: substituted and unsubstituted Taddols,[23] diphenyl(3-methyl-2-indolyl)phosphine,[16a] diisopropyl-(3-methyl-2-indolyl)phosphine,[16a] IndolPhos ligands **1a**−**f**,[16a,b] Taddol-based IndolPhos ligands **2a**,**b**,[16c] 3,7-dimethylindole.[24] Melting points were recorded on a Gallenkamp melting point

(23) Seebach, D.; Beck, A. K.; Heckel, A. *Angew. Chem., Int. Ed.* **2001**, *40*, 92–138.
(24) Dobbs, A. P.; Voyle, M.; Whittall, N. *Synlett* **1999**, 1594–1596.

apparatus and are uncorrected. NMR spectra (^{1}H, ^{31}P, and ^{13}C) were measured on a Varian INOVA 500 MHz. Optical rotations were determined on a Perkin-Elmer 241 polarimeter. High-resolution mass spectra were recorded on a JEOL JMS SX/SX102A four-sector mass spectrometer; for FAB-MS 3-nitrobenzyl alcohol was used as matrix. Chiral GC separations were conducted on an Interscience Focus GC (FID detector) with a Supelco BETA DEX 225 column (0.25 mm × 30 m) or an Astec Chiraldex A-TA column (0.25 mm × 30 m).

General Procedure for the Synthesis of Taddol Phosphorochloridites. The desired Taddol was azeotropically dried prior to use by co-evaporation with PhMe. To a solution of Et_3N (4.00 mmol) in THF (10 mL) was added subsequently PCl_3 (2.08 mmol) and a solution of the corresponding Taddol (1.98 mmol) in THF (10 mL) at −78 °C. The mixture was stirred for 30 min at −78 °C and then allowed to warm to rt. The resulting white suspension was filtered over Celite, and the filtrate was concentrated *in vacuo* to obtain a white solid in quantitative yield, which was used without further purification.

Synthesis of Diphenyl(3,7-dimethyl-2-indolyl)phosphine. To a solution of 3,7-dimethylindole (0.93 g, 6.4 mmol) in THF (20 mL) was added dropwise 2.7 mL of *n*-BuLi (2.5 M in hexanes) at −78 °C. The resulting deep red solution was stirred at −78 °C for 20 min. Carbon dioxide was bubbled through the mixture for 10 min, which was allowed to warm to room temperature, and the solvent was removed *in vacuo*. The resulting residue was dissolved in THF (20 mL) to give a clear solution, which was cooled to −78 °C. To this solution was added 4.2 mL of *t*-BuLi (1.6 M in pentanes), and the resulting orange solution was stirred at −78 °C for 1 h. Chlorodiphenylphosphine (1.15 mL, 6.4 mmol) was added, and the reaction mixture was stirred for 16 h, allowing it to warm to room temperature. The resulting yellow solution was washed with 20 mL of degassed saturated aqueous NH_4Cl. The organic layer was dried over $MgSO_4$ and filtered, and the solvent was removed *in vacuo*. The crude oil was purified by SiO_2 column chromatography (5% EtOAc in hexane) to give an off-white solid. Yield: 1.13 g (53%). Mp = 119.3 °C. ^{1}H NMR (500 MHz; $CDCl_3$; 298 K): δ 7.47 (d, J = 7.4 Hz, 1H), 7.38−7.35 (m, 10H), 7.06 (t, J = 7.5 Hz, 1H), 7.00 (d, J = 7.0 Hz, 1H), 2.46 (s, 3H), 2.30 (s, 3H) ppm. ^{13}C NMR (126 MHz; $CDCl_3$; 298 K): δ 137.8, 136.4 (d, J_{CP} = 9.0 Hz), 133.2, 133.0, 128.93, 128.88, 126.7 (d, J_{CP} = 18.4 Hz), 123.7, 122.9 (d, J_{CP} = 27.2 Hz), 120.2, 119.7, 117.1 (d, J_{CP} = 1.6 Hz), 16.5, 10.1 (d, J_{CP} = 11.1 Hz) ppm. ^{31}P NMR (202 MHz; $CDCl_3$; 298 K): δ −31.56 (s) ppm. HRMS (FAB): calcd for $[M + H]^+$ $C_{22}H_{21}NP$, 330.1412; found, 330.1417.

Synthesis of Taddol-Based IndolPhos Ligand 2c. To a solution of di-*o*-tolyl(3-methyl-2-indolyl)phosphine (0.166 g, 0.48 mmol) in THF (5 mL) was added dropwise 0.20 mL of *n*-BuLi (2.5 M in hexanes) at −78 °C. The resulting yellow solution was stirred for 0.5 h at −78 °C, after which a solution of the phosphorochloridite derived from (4*R*,5*R*)-2,2-dimethyl-α,α,α′,α′-tetraphenyl-1,3-dioxolane-4,5-dimethanol (0.256 g, 0.48 mmol) in THF (5 mL) was added. The reaction mixture was stirred overnight, allowing it to warm to room temperature. The resulting pale yellow solution was evaporated to dryness, and the resulting residue was purified by flash SiO_2 column chromatography (2% EtOAc in hexane) to give a white solid. Yield: 0.258 g (64%). α_D^{22} = +113.2 (*c* 1.0, $CHCl_3$). Mp = 127.5 °C. ^{1}H NMR (500 MHz; $CDCl_3$; 223 K): δ 8.81 (d, J = 8.0 Hz, 0.4H), 8.67 (d, J = 8.8 Hz, 0.6H), 7.85 (br s, 1H), 7.69 (d, J = 8.0 Hz, 0.6H), 7.63 (m, 3.4H), 7.55 (t, J = 7.8 Hz, 1H), 7.45 (d, J = 6.9 Hz, 2H), 7.38−7.08 (m, 21H), 6.91−6.88 (m, 1H), 6.77 (dd, J = 7.6, 3.9 Hz, 1H), 6.41 (br s, 1H), 5.42 (d, J = 8.1 Hz, 0.4H), 5.28 (dd, J = 8.3, 2.1 Hz, 0.6H), 4.93 (d, J = 8.4 Hz, 0.4H), 4.91 (d, J = 8.4 Hz, 0.6H), 2.26 (s, 1.2H), 2.24 (s, 1.8H), 2.07 (s, 3H), 1.65 (s, 3H), 1.59 (s, 1.2H), 1.50 (s, 1.8H), 0.22 (s, 3H) ppm. ^{13}C NMR (126 MHz; $CDCl_3$; 298 K): δ 146.2, 145.1, 140.9, 138.6, 133.1, 130.2 (d, J_{CP} = 5.0 Hz), 129.1, 128.4, 128.2, 127.4, 127.33, 127.31, 127.27, 123.4, 121.2, 118.9, 116.4, 112.2, 83.2 (d, J_{CP} = 9.5 Hz), 83.2, 82.8, 58.5, 57.4, 27.8, 25.4, 21.3 (d, J_{CP} = 20.1 Hz) ppm. ^{31}P NMR (202 MHz; $CDCl_3$; 223 K): δ 141.10 (d, J = 218.4 Hz, 0.4P), 139.89 (d, J = 215.7 Hz, 0.6P), −39.15 (d, J = 216.3 Hz, 0.6P), −42.14 (d, J = 218.2 Hz, 0.4P) ppm. HRMS (FAB): calcd for $[M + H]^+$ $C_{54}H_{50}NO_4P_2$, 838.3215; found, 838.3207.

Synthesis of Taddol-Based IndolPhos Ligand 2d. To a solution of diphenyl(3-methyl-2-indolyl)phosphine (0.209 g, 0.66 mmol) in THF (5 mL) was added dropwise 0.28 mL of *n*-BuLi (2.5 M in hexanes) at −78 °C. The resulting yellow solution was stirred for 0.5 h at −78 °C, after which a solution of the phosphorochloridite derived from (4*R*,5*R*)-2,2-dimethyl-α,α,α′,α′-tetrakis(3,5-dimethylphenyl)-1,3-dioxolane-4,5-dimethanol (0.427 g, 0.66 mmol) in THF (5 mL) was added. The reaction mixture was stirred overnight, allowing it to warm to room temperature. The resulting pale yellow solution was evaporated to dryness, and the resulting residue was purified by flash SiO_2 column chromatography (3% EtOAc in hexane) to give a white solid. Yield: 0.372 g (61%). α_D^{22} = +97.6 (*c* 1.0, $CHCl_3$). Mp = 163.4 °C. ^{1}H NMR (500 MHz; $CDCl_3$; 298 K): δ 8.84 (d, J = 8.3 Hz, 1H), 7.64 (d, J = 7.9 Hz, 1H), 7.52 (t, J = 7.7 Hz, 1H), 7.44 (s, 2H), 7.39−7.26 (m, 14H), 7.16 (s, 4H), 6.82 (d, J = 7.3 Hz, 2H), 6.76 (s, 1H), 5.41 (dd, J = 8.2, 2.9 Hz, 1H), 5.00 (d, J = 8.4 Hz, 1H), 2.27 (s, 6H), 2.22 (s, 6H), 2.13 (s, 6H), 2.07 (s, 6H), 1.75 (s, 3H), 1.66 (s, 3H), 0.39 (s, 3H) ppm. ^{13}C NMR (126 MHz; $CDCl_3$; 298 K): δ 146.3, 145.0, 141.2, 140.9, 139.0, 137.3 (d, J_{CP} = 8.0 Hz), 136.9, 136.3, 135.0, 133.2, 132.5 (d, J_{CP} = 18.5 Hz), 131.9 (d, J_{CP} = 18.4 Hz), 129.3 (d, J_{CP} = 4.4 Hz), 128.9, 128.7, 128.5 (d, J_{CP} = 6.1 Hz), 128.3 (d, J_{CP} = 5.8 Hz), 128.1, 128.0, 127.7, 126.9, 126.5, 125.9 (d, J_{CP} = 3.3 Hz), 125.2, 124.7, 123.1, 121.5, 119.1, 117.3, 111.8, 84.1, 84.0, 83.8, 83.6, 82.2 (d, J_{CP} = 5.4 Hz), 28.1, 25.5, 21.7, 21.68, 21.65, 21.5, 10.6 ppm. ^{31}P NMR (202 MHz; $CDCl_3$; 298 K): δ 140.83 (d, J = 209.9 Hz, 1P), −28.73 (d, J = 210.4 Hz, 1P) ppm. HRMS (FAB): calcd for $[M + H]^+$ $C_{60}H_{62}NO_4P_2$, 922.4154; found, 922.4157.

Synthesis of Taddol-Based IndolPhos Ligand 2e. To a solution of diisopropyl(3-methyl-2-indolyl)phosphine (0.247 g, 1.00 mmol) in THF (10 mL) was added dropwise 0.42 mL of *n*-BuLi (2.5 M in hexanes) at −78 °C. The resulting yellow solution was stirred for 0.5 h at −78 °C, after which a solution of the phosphorochloridite derived from (4*R*,5*R*)-2,2-dimethyl-α,α,α′,α′-tetrakis(3,5-dimethylphenyl)-1,3-dioxolane-4,5-dimethanol (0.643 g, 1.05 mmol) in THF (10 mL) was added. The reaction mixture was stirred overnight, allowing it to warm to room temperature. The resulting pale yellow solution was evaporated to dryness, and the resulting residue was purified by flash SiO_2 column chromatography (2% EtOAc in hexane) to give a white solid. Yield: 0.580 g (68%). α_D^{22} = −93.6 (*c* 1.0, $CHCl_3$). Mp = 133.3 °C. ^{1}H NMR (500 MHz; $CDCl_3$; 318 K): δ 8.47 (d, J = 8.5 Hz, 1H), 7.57 (d, J = 7.9 Hz, 1H), 7.46 (s, 2H), 7.29 (t, J = 7.2 Hz, 1H), 7.23 (t, J = 7.4 Hz, 1H), 7.12 (s, 2H), 7.10 (s, 2H), 6.97 (s, 2H), 6.95 (s, 1H), 6.86 (s, 1H), 6.82 (s, 1H), 6.81 (s, 1H), 5.74 (dd, J = 8.0, 4.3 Hz, 1H), 4.99 (d, J = 8.2 Hz, 1H), 2.46 (s, 3H), 2.37 (br m, 1H), 2.34 (s, 6H), 2.29 (br m, 1H), 2.24 (s, 6H), 2.23 (s, 6H), 2.19 (s, 6H), 1.43 (s, 3H), 1.08−1.03 (m, 3H), 0.92−0.82 (m, 6H), 0.58−0.53 (m, 3H), 0.48 (s, 3H) ppm. ^{13}C NMR (126 MHz; $CDCl_3$; 298 K): δ 145.5 (d, J_{CP} = 2.2 Hz), 142.0, 141.6, 139.0, 137.2, 136.9, 136.8, 136.1, 129.5, 129.3, 128.9, 127.5, 126.5, 125.9, 125.2, 122.9, 121.2, 119.2, 117.6, 112.4, 110.7, 83.3, 83.2, 82.9, 27.9, 26.1, 25.5, 24.6, 21.8, 21.7, 21.6, 20.5 (d, J_{CP} = 19.5 Hz), 19.8 (d, J_{CP} = 7.8 Hz), 11.3 (d, J_{CP} = 15.8 Hz) ppm. ^{31}P NMR (202 MHz; $CDCl_3$; 318 K): δ 139.89 (d, J = 61.3 Hz, 1P), −7.67 (d, J = 58.0 Hz, 1P) ppm. HRMS (FAB): calcd for $[M + H]^+$ $C_{54}H_{66}NO_4P_2$, 854.4467; found, 854.4484.

Synthesis of Taddol-Based IndolPhos Ligand 2f. To a solution of diphenyl(3-methyl-2-indolyl)phosphine (0.196 g, 0.62 mmol) in THF (5 mL) was added dropwise 0.26 mL of *n*-BuLi (2.5 M in hexanes) at −78 °C. The resulting yellow solution was stirred for 0.5 h at −78 °C, after which a solution of the phosphorochloridite derived from (4*R*,5*R*)-2,2-dimethyl-α,α,α′,α′-tetrakis[3,5-bis(trifluoromethyl)phenyl]-1,3-dioxolane-4,5-dimethanol (0.800 g, 0.74 mmol) in THF (5 mL) was added. The reaction mixture was stirred overnight, allowing it to warm to room temperature. The resulting pale yellow solution was evaporated to dryness, and the resulting residue was purified by flash SiO_2 column

chromatography (4% EtOAc in hexane) to give a white solid. Yield: 0.352 g (45%). $\alpha_D^{22} = -60.0$ (*c* 1.0, $CHCl_3$). Mp = 105.4 °C. ^{1}H NMR (500 MHz; $CDCl_3$; 298 K): δ 8.31 (s, 2H), 8.23 (s, 1H), 7.99 (s, 2H), 7.93 (s, 1H), 7.91 (s, 2H), 7.86 (s, 1H), 7.83 (s, 3H), 7.78 (s, 1H), 7.66 (d, J = 7.8 Hz, 1H), 7.49 (t, J = 7.8 Hz, 1H), 7.40 (t, J = 7.5 Hz, 1H), 7.31 (br s, 3H), 7.27−7.19 (m, 5H), 7.12 (t, J = 7.5 Hz, 2H), 5.43 (dd, J = 8.2, 3.4 Hz, 1H), 4.75 (d, J = 8.5 Hz, 1H), 1.71 (s, 3H), 1.58 (s, 3H), 0.46 (s, 3H) ppm. ^{13}C NMR (126 MHz; $CDCl_3$; 298 K): δ 145.9, 145.2 (d, J_{CP} = 2.4 Hz), 141.9, 141.6, 138.6, 134.2 (t, J_{CF} = 6.7 Hz), 133.9 (t, J_{CF} = 5.4 Hz), 133.7, 132.9 (d, J_{CP} = 10.7 Hz), 132.6, 132.4, 132.3 (d, J_{CP} = 3.7 Hz), 132.1 (d, J_{CP} = 3.0 Hz), 132.0, 131.9, 131.8, 131.7, 131.5, 131.3, 129.2, 128.73, 128.67, 128.65, 128.60, 128.5, 127.1, 126.4, 126.3, 126.3, 126.2, 124.9, 124.20, 124.17, 124.12, 124.0, 123.5, 122.8, 122.7, 122.03, 122.00, 121.9, 121.8, 120.2, 119.9, 119.83, 119.77, 119.6, 114.6, 114.1, 82.8, 82.2 (d, J_{CP} = 11.1 Hz), 81.41, 81.36, 81.2, 27.2, 25.6, 10.40 ppm. ^{31}P NMR (202 MHz; $CDCl_3$; 298 K): δ 138.93 (d, J = 198.9 Hz, 1P), −26.10 (d, J = 198.8 Hz, 1P) ppm. HRMS (FAB) calcd for $[M + H]^+$ $C_{60}H_{38}F_{24}NO_4P_4$, 1354.1893; found, 1354.1904.

Synthesis of Taddol-Based IndolPhos Ligand 2g. To a solution of diphenyl(3,7-dimethyl-2-indolyl)phosphine (0.310 g, 0.94 mmol) in THF (10 mL) was added dropwise 0.40 mL of *n*-BuLi (2.5 M in hexanes) at −78 °C. The resulting yellow solution was stirred for 0.5 h at −78 °C, after which a solution of the phosphorochloridite derived from (4*R*,5*R*)-2,2-dimethyl-α,α,α′,α′-tetraphenyl-1,3-dioxolane-4,5-dimethanol (0.525 g, 0.99 mmol) in THF (5 mL) was added. The reaction mixture was stirred overnight, allowing it to warm to room temperature. The resulting pale yellow solution was evaporated to dryness, and the resulting residue was purified by flash SiO_2 column chromatography (3% EtOAc in hexane) to give a white solid. Yield: 0.327 g (42%). $\alpha_D^{22} = +94.4$ (*c* 1.0, $CHCl_3$). Mp = 189.1 °C. ^{1}H NMR (500 MHz; $CDCl_3$; 233 K): δ 7.83 (br s, 2H), 7.58 (t, J = 7.2 Hz, 2H), 7.42 (t, J = 6.7 Hz, 4H), 7.38−7.33 (m, 8H), 7.28−7.21 (m, 8H), 7.12 (t, J = 7.5 Hz, 2H), 7.05 (ddd, J = 21.3, 14.5, 7.1 Hz, 5H), 6.87 (t, J = 7.7 Hz, 2H), 5.40 (dd, J = 8.3, 2.5 Hz, 1H), 5.22 (d, J = 8.4 Hz, 1H), 1.94 (s, 1.5H), 1.92 (s, 1.5H), 1.69 (s, 3H), 1.51 (s, 3H), 0.12 (s, 3H) ppm. ^{13}C NMR (126 MHz; $CDCl_3$; 298 K): δ 147.0 141.9, 140.7, 136.6 (t, J_{CP} = 16.1 Hz), 132.1, 131.7 (d, J_{CP} = 18.3 Hz), 129.8 (d, J_{CP} = 8.0 Hz), 129.0 (d, J_{CP} = 6.2 Hz), 128.3, 127.7, 127.3, 121.1, 116.8, 112.1, 84.8, 84.3, 83.2, 83.1, 82.6, 27.9, 24.9, 11.5 ppm. ^{31}P NMR (202 MHz; $CDCl_3$; 233 K): δ 140.88 (d, J = 6.7 Hz, 1P), −23.08 (d, J = 6.1 Hz, 1P) ppm. HRMS (FAB): calcd for $[M + H]^+$ $C_{53}H_{48}NO_4P_2$, 824.3059; found, 824.3054.

General Procedure for Asymmetric Hydroformylation. The experiments were carried out in a stainless steel autoclave (150 mL) charged with an insert suitable for eight reaction vessels (including Teflon mini-stirring bars) for conducting parallel reactions. Styrene was filtered freshly over basic alumina to remove possible peroxide impurities. The autoclave was charged with 1.0 μmol of $[Rh(acac)(CO)_2]$, 2.0 μmol of ligand, 1.0 mmol of substrate, and 0.50 mmol of internal standard (decane for styrene and allyl cyanide, heptane for vinyl acetate) in a total volume of 1.0 mL using toluene as solvent. Before starting the catalytic reactions, the charged autoclave was purged three times with 15 bar of syngas (CO/H_2 = 1:1) and then pressurized at 20 bar (CO/H_2 = 1:1). The reaction mixtures were stirred at 40 or 70 °C for 20 h. After catalysis the pressure was reduced to 1.0 bar, and the conversion and b/l ratio were checked by GC (BPX35 column, FID detector). The enantiomeric purity was determined by chiral GC. For styrene: Supelco BETA DEX 225 column; initial temperature = 100 °C for 5 min, then 4 °C/min to 160 °C; $t_R(S)$ = 11.27 min and $t_R(R)$ = 11.45 min. For vinyl acetate: Supelco BETA DEX 225 column; initial temperature = 100 °C for 5 min, then 4 °C/min to 160 °C; $t_R(S)$ = 6.14 min and $t_R(R)$ = 7.85 min. For allyl cyanide: Astec Chiraldex A-TA column; initial temperature = 90 °C for 7 min, then 5 °C/min to 180 °C; $t_R(S)$ = 16.29 min and $t_R(R)$ = 16.75 min.

Kinetic Gas-Uptake Measurements. The experiments were carried out in an AMTEC SPR16 consisting of 16 parallel reactors equipped with temperature and pressure sensors and a mass flow controller. The apparatus is suited for monitoring gas-uptake profiles during the catalytic reactions. The autoclaves were heated to 110 °C and flushed with argon (22 bar) five times. Next, the reactors were cooled to 25 °C and flushed again with argon (22 bar) five times. The autoclaves were charged with the appropriate amount of $[Rh(acac)(CO)_2]$, ligand, substrate, and internal standard in 5.00 mL of toluene under argon. The reactors were heated to 40 °C and pressurized to the desired pressure with CO/H_2 (1:1), and the pressure was kept constant during the whole reaction. The reaction mixtures were stirred at 40 °C for 17 h, and the syngas uptake was monitored and recorded for every reactor. After catalysis the pressure was reduced to 2.0 bar, and samples were taken for GC and chiral GC analysis.

High-Pressure NMR Experiments. In a typical experiment a 5 mm sapphire high-pressure NMR tube was filled with a solution of $[Rh(acac)(CO)_2]$ (4.0 mg, 0.016 mmol), ligand (0.017 mmol), and benzene-d_6 (0.5 mL) under an argon atmosphere. Formation of the acac complex [Rh(acac)(**L**)] was checked by NMR. The tube was then purged three times with 5 bar of CO/H_2 (1:1), pressurized with 5 bar of CO/H_2 (1:1), and left for 16 h at 50 °C. After cooling to room temperature the NMR spectra were recorded at the desired temperature.

High-Pressure *in Situ* IR Spectroscopy. In a typical experiment a 50 mL HP IR autoclave was filled with a solution of ligand (0.030 mmol) in cyclohexane (15 mL). The autoclave was purged three times with 15 bar of CO/H_2 (1:1), pressurized with 20 bar of CO/H_2 (1:1), and heated at 40 °C under stirring, and a background spectrum was recorded. A solution of $[Rh(acac)(CO)_2]$ (3.9 mg, 0.015 mmol) in cyclohexane (1 mL), previously charged into the reservoir of the autoclave, was added to the reaction mixture by overpressure. After complete conversion to the hydridobiscarbonyl rhodium species a solution of vinyl acetate (0.28 mL, 3.0 mmol) in cyclohexane (1 mL), previously charged into the reservoir of the autoclave, was added to the reaction mixture by overpressure. The IR spectra were recorded at 40 °C.

DFT Calculations. The geometry optimizations were carried out with the Turbomole program[25] coupled to the PQS Baker optimizer.[26] The geometries were optimized as minima at the ri-DFT BP86[27] level using the SV(P) basis set[28] on all atoms. We applied the BOpt script package developed by Prof. Peter H. M. Budzelaar to facilitate all data evaluation processes.[29] The obtained stationary points (minima) were characterized by vibrational analysis (numerical frequencies); ZPE and gas phase thermal corrections (entropy and enthalpy, 298 K, 1 bar) from these analyses were calculated according to standard formulas of statistical thermodynamics. The thus obtained (free) energies (kcal mol^{-1}) are reported in Table 6.

Acknowledgment. This work was supported by NRSC-C and the European Union (RTN Revcat MRTN-CT-2006-035866). We thank V. Bocokic for assistance with the high-pressure IR experiments and Dr. J. I. van der Vlugt for fruitful discussions.

Supporting Information Available: High-pressure ^{1}H and ^{31}P NMR spectra for the hydridobiscarbonyl rhodium complexes, and NMR spectra for all new ligands and deuterioformylation products. This material is available free of charge via the Internet at http://pubs.acs.org.

(25) (a) Ahlrichs, R. *Turbomole Version 5*; Theoretical Chemistry Group, University of Karlsruhe, 2002. (b) Schäfer, A.; Huber, C.; Ahlrichs, R. *J. Chem. Phys.* **1994**, *100*, 5829–5835.

(26) (a) *PQS version 2.4*; Parallel Quantum Solutions: Fayettevile, AR, 2001 (the Baker optimizer is available separately from PQS upon request). (b) Baker, J. *J. Comput. Chem.* **1986**, *7*, 385–395.

(27) (a) Becke, A. D. *Phys. Rev. A: Gen. Phys.* **1988**, *38*, 3098–3100. (b) Perdew, J. P. *Phys. Rev. B* **1986**, *33*, 8822–8824.

(28) Schäfer, A.; Horn, H.; Ahlrichs, R. *J. Chem. Phys.* **1992**, *97*, 2571–2577.

(29) Budzelaar, P. H. M. *J. Comput. Chem.* **2007**, *28*, 2226–2236.